Catalysis Today 144 (2009) 273–277

Contents lists available at ScienceDirect

Catalysis Today

journal homepage: www.elsevier.com/locate/cattod

The structure and activity of Pt_6 particles in ZSM-5 type zeolites

M.N. Mikhailov [a,b,*], I.V. Mishin [a], L.M. Kustov [a], V.Z. Mordkovich [b]

[a] N.D. Zelinsky Institute of Organic Chemistry, Russian Academy of Sciences, Leninsky prospect 47, 119991 Moscow, Russian Federation
[b] United Research and Development Center, Leninsky prospect 55/1, bld. 2, 119333 Moscow, Russian Federation

ARTICLE INFO

Article history:
Available online 16 December 2008

Keywords:
ZSM-5 zeolite
Pt particle
Active sites
Alkane isomerization
DFT

ABSTRACT

Density functional theory was applied to investigate the nature of active sites formed by the interaction of a Pt_6 guest particle with the silicalite and H-form of ZSM-5 as the host zeolites. Interaction of metal cluster with silicalite shows a slight stabilization (36 kJ/mol) and formation of a negatively charged Pt entity. When a metal particle is arranged in the channel of H-form substantial stabilization (187 kJ/mol) and generation of an oxidized Pt_6H^+ species are observed. The formation of an active site includes interaction between a platinum particle and an acid site accompanied by the suppression of zeolite acidity. The suggestion is made that the alkane transformation on supported platinum particles proceeds *via* metal–cyclobutane and metal–carbene intermediates and does not need the direct involvement of acid sites. The difference in catalytic behavior of the Pt_6/HZSM-5 and Pt_6/ZSM-5 systems is discussed.

1. Introduction

Conventional description of bifunctional Pt/zeolite catalysts implies the independent functioning of metal and acid sites [1,2]. According to this concept, hydrogenation and dehydrogenation occur on a metal particle, whereas isomerization proceeds on an acid site. This picture suggests two different kinds of sites and a negligible mutual influence among metal and acid sites [3]. However, numerous experimental and theoretical studies indicate a strong interaction between metal particle and acid surfaces of zeolites. In particular, Freund and coworkers [4,5] presented evidence that on introducing rhodium particles on the alumina surface the concentration of the surface hydroxyls decreases, whereas Rh 3d-bands shift to higher binding energies. That results in the oxidation and stabilization of supported metal particles:

$$Rh_n{}^0 + OH_s{}^- \rightarrow Rh_n{}^+ + H_{ads} + O_s{}^{2-},$$

where Rh_n is the supported metal particle, $OH_s{}^-$ is the surface hydroxyl, H_{ads} is the adsorbed hydrogen atom, and $O_s{}^{2-}$ is the surface anion of the oxide support.

XPS data indicate that metal clusters supported on acid oxides are electron deficient [6] and the deficiency increases with acidity [7]. Electron deficiency of metal particles is also confirmed by the frequency shift in the infrared spectra of adsorbed CO [8–10]. Recently, Murzin et al. [11,12] reported the relation between the changes in the electronic structure of supported platinum particles and the acid site strength of zeolites. In the presence of platinum the concentration of acid sites decreases and in some cases both Brønsted and Lewis acidities are completely suppressed. The DFT calculations by Rösch [13–16] provided evidence that the interaction between metal particles and H form of X zeolite leads to transfer of hydrogen atoms of hydroxyls onto the metal surface and to the oxidation of the metal particle. The density functional theory [17] indicates that interaction of platinum atom with HZSM-5 zeolite results in transfer of electron density from oxygen to metal atom.

We reported earlier [18] that on introducing the platinum cluster in the high-silica zeolite the reverse hydrogen spillover from the Brønsted acid site (BAS) onto the metal surface occurs. This leads to the oxidation of the metal particle and suppression of Brønsted acidity of the zeolite support. Adsorption on basic sites of the support favors the formation of electron-enriched metal clusters. By analyzing possible pathways for alkane isomerization [19] we proposed the mechanism that involves a metal–cyclobutane and metal-carbene species and does not imply Brønsted acidity as the driving force of the reaction. However, the catalytic significance of the Brønsted proton transferred onto platinum particle is unclear. To clarify the effect of the Brønsted acid site (BAS) on the activity of platinum species towards C-C bond cleavage and its selectivity for isomerization/cracking, we calculated the key steps of alkane transformation over Pt_6/HZSM-5 and Pt_6/ZSM-5 systems. The first system is a Pt_6 guest particle in acidic ZSM-5 zeolite, whereas the second one represents Pt_6 cluster

---

* Corresponding author at: N.D. Zelinsky Institute of Organic Chemistry, Russian Academy of Sciences, 119991 Moscow, Leninsky prospect 47, Russian Federation.
E-mail address: mik@ioc.ac.ru (M.N. Mikhailov).

0920-5861/$ – see front matter © 2008 Elsevier B.V. All rights reserved.
doi:10.1016/j.cattod.2008.10.042

arranged in proton-free ZSM-5 zeolite (silicalite). By comparing activity and selectivity of Pt_6 particles in these systems it is possible to throw some light on the sources of high activity of platinum supported acidic zeolites.

2. Computational details

To model the fragment of ZSM-5 zeolite, the cluster approach was used. Cluster modeling silicalite structure includes fifteen Si atoms while the cluster representing HZSM-5 fragment contains fourteen Si atoms and one Al atom. Both clusters are based on two ten-membered rings extracted from the straight channel of the ZSM-5 zeolite. The broken bonds (Si–O and Al–O) were saturated with hydrogens placed at 1.6 and 1.5 Å along Al–O and Si–O bonds, respectively. All terminal hydrogens were fixed during the geometry optimization. The obtained clusters have the stoichiometry $Si_{15}O_{18}H_{24}$ and $HAlSi_{14}O_{18}H_{24}$. To model interaction between platinum and zeolite frameworks the Pt_6 particle was placed inside the clusters. The cluster electronic structure was computed at the density functional theory (DFT) level using the Becke's three parameters exchange functional (B3) [20] combined with the Lee-Yang-Parr (LYP) [21] and Vosko-Wilk-Nusair (VWN5) [22] correlation functionals. The SBK effective core potential [23] and corresponding basis set augmented with polarization functions were used on all atoms. All clusters were fully optimized without symmetry constraints. The transition state structures were verified by performing normal mode analysis. On calculating the frequencies the atomic masses of 100,000 for the terminal hydrogen atoms were applied. The calculations were performed with the PC GAMESS [24,25] program package. The charges were calculated using natural populations [26] and density of states spectra were obtained with the help of AOMix package [27,28].

3. Results and discussion

Table 1
Natural charges in the clusters modeling HZSM-5, ZSM-5, Pt_6/HZSM-5 and Pt_6/ZSM-5 structures.

Atom(s)	HZSM-5	ZSM-5	Pt_6H/ZSM-5	Pt_6/ZSM-5
H[a]	−6.57	−6.43	−6.46	−6.33
O[a]	−22.30	−23.53	−22.35	−23.55
Si[a]	27.63	29.96	27.73	30.07
Al	1.86	–	1.90	–
Pt_6	–	–	0.54	−0.19
O (BAS)	−1.17	–	−1.37	–
H (BAS)	0.55	–	0.01	–

[a] Sum of the natural charges on atoms.

Table 2
Spin multiplicity (*M*), adsorption energy (E_{ads}), ionization energy (*IE*), electron affinity (*EA*), Fukui function (*f*), chemical potential (μ), hardness (η) and local hardness (η') for the bare Pt_6 cluster and the Pt_6 particles incorporated in silicalite and HZSM-5 zeolite.

Cluster	*M*	E_{ads} (kJ/mol)	*IE*[a] (eV)	*EA*[a] (eV)	*f*	μ (eV)	η (eV)	η' (eV)
Pt_6	9	–	6.94	2.51	1.0	−4.73	2.22	2.22
Pt_6H/ZSM-5	3	187	5.59	1.82	0.81	−3.71	1.89	1.53
Pt_6H/ZSM-5	1	178	5.53	1.84	0.79	−3.69	1.85	1.46
Pt_6/ZSM-5	3	36	5.60	1.55	0.87	−3.58	2.03	1.77

[a] Ionization energy (electron affinity) was calculated as the difference in energy between the positively (negatively) charged and neutral clusters. The spin multiplicities for the Pt_6^+ and Pt_6^- clusters were found to be 6 and 8, correspondingly.

The optimized clusters modeling a platinum particle occluded in the channels of silicalite (Pt_6/ZSM-5) and HZSM-5 zeolite (Pt_6/HZSM-5) are presented in Fig. 1. Natural charges on atoms are given in Table 1. The energetic parameters for the bare Pt_6 cluster and the Pt_6 particle incorporated in silicalite and HZSM-5 zeolite are collected in Table 2. Interaction between the silicalite and the Pt_6 particle (electronic configuration $5d^{9.41}6\ s^{0.55}$, distorted octahedron, Pt–Pt distances are 2.63, 2.66 and 2.97 Å) is characterized by the adsorption energy as low as 36 kJ/mol. In response to the interaction, Pt5–Pt6 and Pt3–Pt4 distances increase by 0.92 and 1.36 Å, correspondingly, whereas Pt1–Pt2 distance decreases by 1.01 Å. This indicates a considerable change in the shape of a Pt_6 particle that stretches along the zeolite channel. The Al–O and Si–O bonds of the zeolite framework change insignificantly (0.01–0.02 Å). The Pt_6 cluster localized in the silicalite channel interacts with the oxygen anions of the lattice (the Pt–O bond distances are 2.3–3.0 Å). Due to this interaction, the electronic density on the platinum particle increases and it charges negatively (Table 1). Adsorption on oxygen anions of the zeolite favors the formation of an electron enriched metal clusters. The reason for the appearance of the negative charge are incoming charges from the nearest Si atoms through the O atoms of the zeolite framework onto the

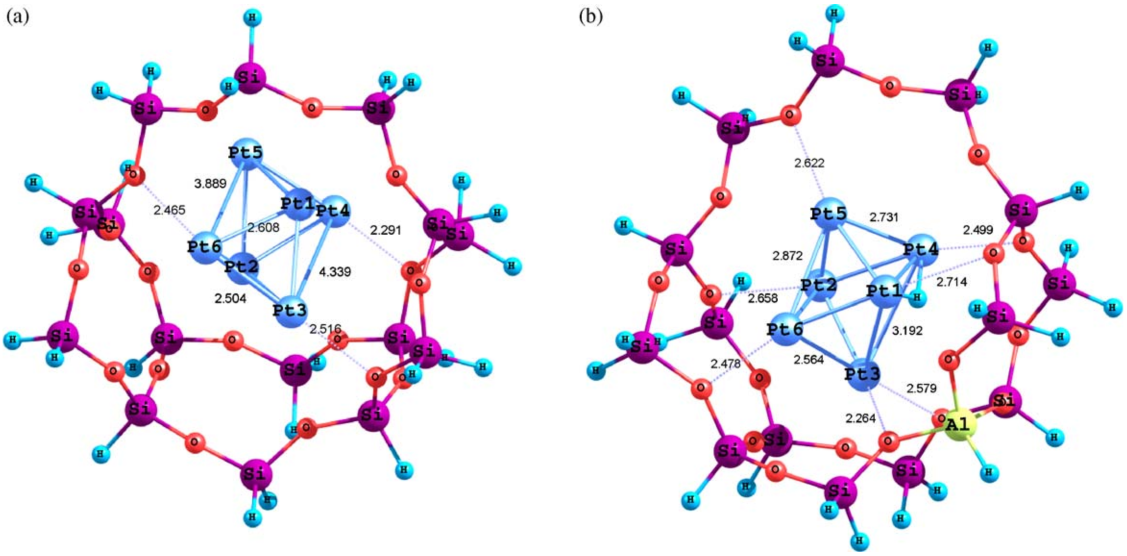

Fig. 1. Optimized clusters (distances in Å) modeling the Pt_6 particle incorporated in silicalite (a) and HZSM-5 zeolite (b).

metal particle whereby the electronic density on Pt 6s orbitals increases and that on Pt 5d orbitals decreases (electronic configuration $\sim 5d^{9.18}6s^{0.81}$).

Interaction of Pt_6 particle with HZSM-5 zeolite is accompanied by the transfer of the Brønsted proton to the metal particle (reverse spillover) and formation of the structure involving Pt_6H^+ particle (Fig. 1b). In Pt_6 cluster adsorbed in HZSM-5 channel, the Pt1–Pt3, Pt3–Pt4 and Pt3–Pt5 bonds lengthen by 0.39, 0.53 and 0.38 Å, respectively. The bond lengths of 1.75 and 1.67 Å for Pt1–H and Pt4–H can be best explained by formation of atomic hydrogen (electronic configuration $1s^{0.99}$) adsorbed on Pt1 and Pt4 atoms. The total charge of the metal particle with the transferred Brønsted proton reaches a value of 0.54. As a result of proton transfer the Pt atoms nearest to the framework Al^{3+} cation are oxidized: Pt1 ($5d^{9.28}6s^{0.63} \rightarrow 5d^{9.12}6s^{0.62}$, charge 0.21) and Pt3 ($5d^{9.34}6s^{0.65} \rightarrow 5d^{9.16}6s^{0.56}$, charge 0.22) atoms. These data are consistent with Pt_6H^+ complex occupying a cation position. A possible mechanism of the proton transfer includes withdrawal of electronic density from the platinum particle onto BAS to generate an anion-radical fragment in the zeolite framework followed by the O–H bond cleavage and the adsorption of a hydrogen atom on the platinum surface. Accordingly, inclusion of platinum particle into acid ZSM-5 zeolite is characterized by much higher energy of 187 kJ/mol compared with 36 kJ/mol for silicalite. All the above data fall into a single pattern in which the presence of platinum in ZSM-5 zeolite suppresses the Brønsted acidity and forms Pt_6H^+ species.

To understand the changes of electronic structure caused by interaction of the Pt_6 particle with zeolite surface, we calculated the density of states of the electronic structures for the bare Pt_6 cluster and the Pt_6 particle incorporated in silicalite and HZSM-5 zeolite. The results are shown in Fig. 2. For the Pt_6/HZSM-5 (singlet state) system only the α-spin states are presented since the β-spin states are identical. The bare Pt_6 cluster has a spin multiplicity of 9. In silicalite, Pt orbitals interact with 2p orbitals of the framework oxygens to stabilize Pt_6 particle in the triplet state. This can be accounted for by the filling of β-valence band at −3.75 eV in the bare Pt_6 particle at the expense of zeolite basic sites. This band shifts towards higher binding energies and merges with conduction bands as depicted in Fig. 2. Singlet-triplet splitting for the Pt_6/ZSM-5 system is 40 kJ/mol. Stabilization of Pt_6 particle by the acid site in the HZSM-5 zeolite decreases the singlet-triplet splitting to a value below 15 kJ/mol. The singlet and triplet states for the Pt_6/HZSM-5 structure are nearly degenerate. Accordingly, the open-shell Pt_6 cluster becomes a closed-shell system.

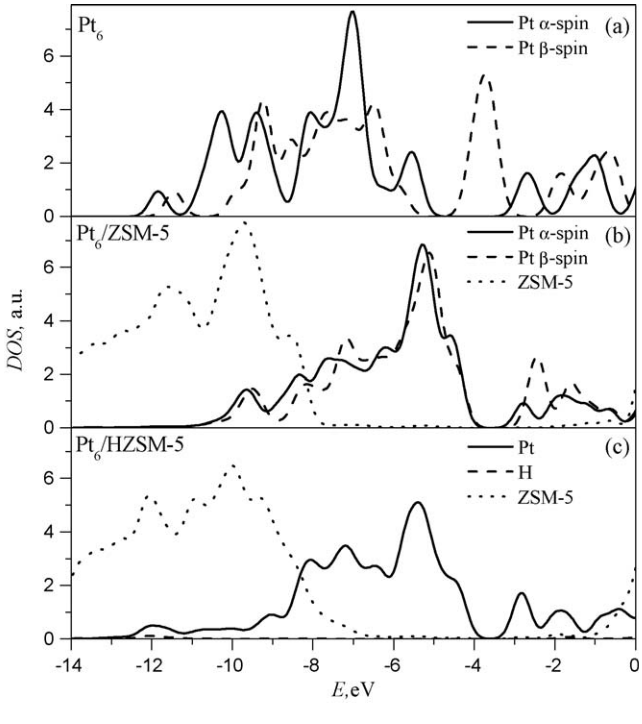

Fig. 2. The density of states for the bare Pt_6 particle (a) and the Pt_6 particles incorporated in silicalite (b) and HZSM-5 zeolite (c).

The Pt_6 particles immobilized in zeolite channels have low ionization energies and electron affinities as compared with the bare Pt_6 particle. Consequently, the presence of platinum cluster in the zeolite decreases the chemical potential and hardness of Pt particles. The chemical potential (μ) and hardness (η) were calculated as

$$\mu = -\frac{IE + EA}{2} \quad \text{and} \quad \eta = \frac{IE - EA}{2},$$

where *IE* is the ionization energy and *EA* is the electron affinity. This reduction is more pronounced for Pt_6/ZSM-5 structure than for Pt_6/HZSM-5. By contrast, a decrease in hardness is more discernible for Pt_6/HZSM-5 system (by 0.33 eV) than for Pt_6/ZSM-5 (by 0.19 eV). Since Pt_6 cluster supported on silicalite is characterized by a higher value of Fukui function, the difference in local hardness between Pt_6/ZSM-5 and Pt_6/HZSM-5 is as high as ca. 0.25 eV. The conduction bands of the bare platinum particle located about −12 to −7 eV (Fig. 2a) shift to lower binding energies to increase the electronic density near the Fermi level for both Pt_6/zeolite structures. Transfer of Brønsted proton onto platinum particle leads to the appearance of the Pt-H bonding (at −12.05 eV) and anti-bonding (at −1.65 eV) bands.

Therefore, on introducing platinum into silicalite only slight stabilization effect (36 kJ/mol) and formation of negatively charged metal cluster are observed. At the same time interaction of Pt_6 particle with BAS is accompanied by transfer of proton onto metal surface and leads to: (1) significant stabilization of Pt_6 cluster, (2) formation of the oxidized species Pt_6H^+, and (3) substantial decrease in the number of Brønsted acid sites or even their complete suppression.

In this context, the nature sites responsible for alkane transformation on bifunctional catalysts can be discussed. According to the conventional concept, one function is a function of an acid catalyst, the other being a function of a hydrogenation-dehydrogenation catalyst. Thus, it is supposed that an alkane is first dehydrogenated on metal sites to the corresponding alkene, which is then isomerized on acid sites into a branched alkene. The branched alkene is subsequently hydrogenated into the branched alkane again on the metal site. However, from the results outlined above, it follows that in the presence of platinum the number of acid sites decreases. Accordingly, the bifunctional mechanism might not be always operative in the alkane isomerization on platinum supported zeolites.

Many more quantum chemical calculations coupled with experimental observations are needed to clarify the bifunctional action of Pt/ZSM-5 systems, but preliminary interpretation can be given as follows. Recent analysis [19] of the key intermediates formed by interaction between alkane and metal particle serves to propose the mechanism of alkane transformation over metal/zeolite catalysts without the direct involvement of acid sites. According to the mechanism (Scheme 1), at the first step, *n*-alkane oxidative addition to the platinum atom results in alkyl surface structure **2**. Then hydrogen transfer from the alkyl fragment of cluster **2** to the platinum surface leads to metal–cyclobutane complex **3**. At the next step, the C–C bond in the metal–cyclobutane derivative is broken to form the surface carbene species coordinatively bound to two platinum atoms and π-

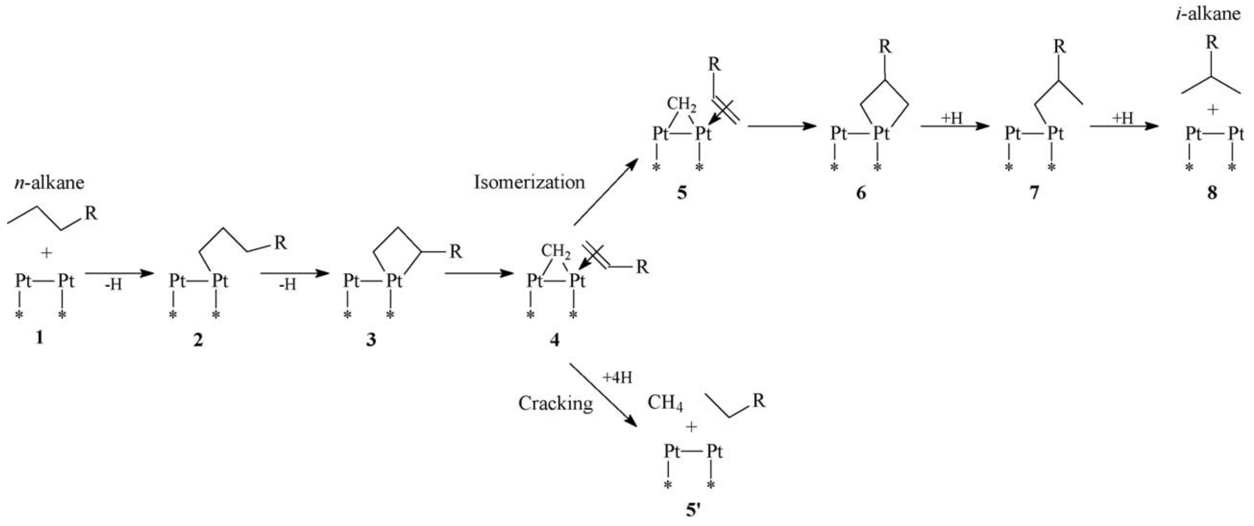

Scheme 1. Alkane transformation on the supported Pt particles.

bonded alkene, structure **4**. Further transformation of complex **4** can proceed either as isomerization or cracking. Isomerization includes rotation of π-bonded alkene and recombination with surface carbene into iso-metal–cyclobutane complex **6**. Finally, the hydrogenation of structure **6** gives *i*-alkane and regenerates the initial platinum cluster. Cracking involves cleavage of C–C bond (step **3** → **4**) followed by migration of adsorbed alkene and subsequent hydrogenation of hydrocarbon fragments.

Now we can try to apply this picture to rationalize the catalytic behaviour of the Pt_6/ZSM-5 and Pt_6/HZSM-5 systems. In view of the absence of BAS in both systems the different catalytic properties can be explained by the differences in electronic structure of Pt_6 particles rather than by variations in acidity of the support. To trace the effect of electronic structure on the activity of catalysts the energy profiles (Fig. 3) for the key steps were calculated in singlet and triplet states. A simplified scheme (Scheme 2) includes C–C bond cleavage in metal–cyclobutane complex **I** to form surface carbene and adsorbed alkene (structure **II**). The activity of catalyst in alkane transformation seems to be a function of the height of the activation barrier of C–C bond cleavage (E_{a1}). The steps governing the selectivity are the recombination of carbene and alkene (step **II** → **I**, activation energy E_{a2}) and alkene desorption (desorption energy E_d). It can be further speculated that alkene migration over the metal surface rather than desorption occurs under conditions of a real catalytic reaction. Since the feasibility of this process is related to the E_d value and the contribution of iso-alkanes increases with decreasing of E_{a2} values, it appears that the isomerization to cracking ratio depends on the value of E_d/E_{a2}. The higher values favor higher contribution of isomerization.

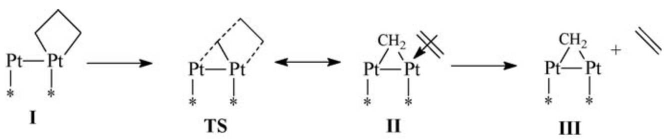

Scheme 2. Key steps of alkane transformation on the supported Pt particles.

On analyzing the energy profile for the Pt_6/HZSM-5 system (Fig. 3a) it is evident that transformation shown on Scheme 2 follows the triplet surface. The singlet surface lies 20–40 kJ/mol above the triplet one and has a similar pattern. Except for the structure **I** the transformation in the Pt_6/ZSM-5 system proceeds on the singlet surface (Fig. 3b). Since the metal–cyclobutane complex in silicalite has the triplet as the ground state with the singlet state located 63 kJ/mol higher, the transformation begins on triplet surface (structure **I**) and passes through the intersection point **SI** on the triplet surface. On comparing the energy profiles for two systems one can see that in the case of silicalite the activation

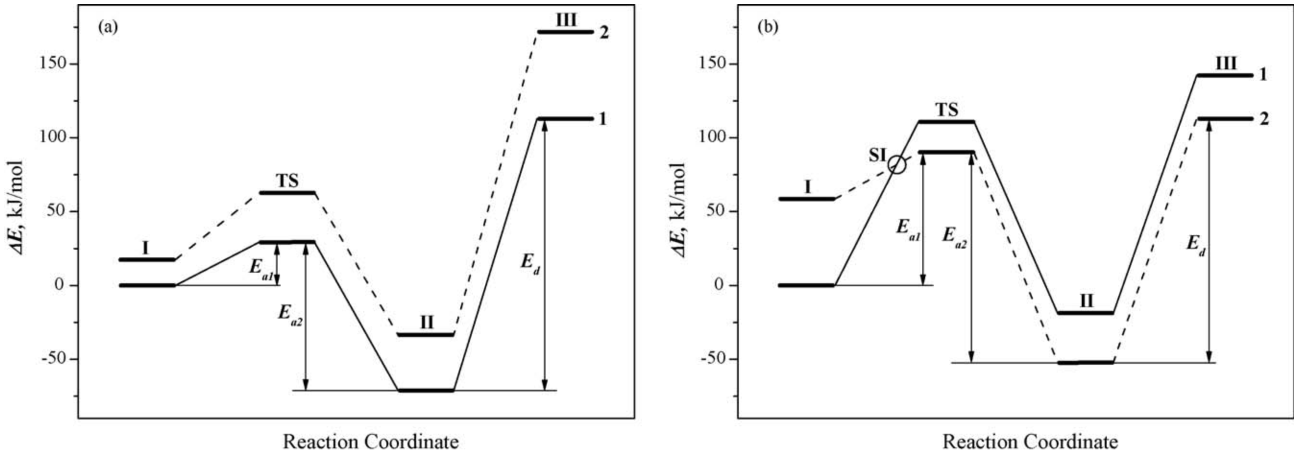

Fig. 3. Energy profiles for the key steps of alkane transformation on Pt_6/HZSM-5 (a) and Pt_6/ZSM-5 (b) catalysts in the triplet (1) and singlet (2) states.

energy for the C–C bond cleavage step (**I** → **II**) is ca. 2.5 times higher than for the H-form. The reason for this can be explained as due to the fact that the Pt_6 particle in H-form has the chemical potential 0.12 eV higher and the hardness 0.25 eV lower compared to the silicalite system.

Now we can try to use E_d/E_{a2} ratio to estimate catalyst selectivity for isomerization and cracking. The energy profiles show that on passing from the H-form to silicalite E_{a2} increases from 100 to 142 kJ/mol while E_d decreases from 184 to 159 kJ/mol. Accordingly, E_d/E_{a2} ratios for the Pt_6/HZSM-5 and Pt_6/ZSM-5 systems are 1.8 and 1.1, correspondingly. It appears therefore that the contribution from isomerization is higher for the H-form. Calculated energies of ethene desorption for the isolated Pt_6^-, Pt_6 and Pt_6^+ clusters indicate that increment in desorption energy for the positively charged species is two times higher than for the negatively charged cluster. Consequently, an acid site plays an important part in the formation of active site in the H-form by generating stable oxidized Pt_6H^+ species.

4. Conclusions

The results outlined above show that the introduction of platinum particle in silicalite and H-form of ZSM-5 zeolite leads to the formation of active sites with different natures. On interacting with silicalite metal cluster slight stabilization and formation of the negatively charged species are observed. The channels of H-form significantly stabilize metal particles generating the oxidized platinum species. The formation of active site includes the interaction between platinum particle and acid site and suppression of support acidity. The suggestion is made that the different catalytic behavior of the Pt_6/HZSM-5 and Pt_6/ZSM-5 systems can be explained in terms of changing chemical potential and hardness of supported platinum particles. The alkane transformation proceeds *via* metal–cyclobutane and metal–carbene intermediates and without the direct involvement of acid sites.

References

[1] P.B. Weisz, E.W. Swegler, Science 126 (1957) 31.
[2] A. Kuhlmann, F. Roessner, W. Schwieger, O. Gravenhorst, T. Selvam, Catal. Today 97 (2004) 303.
[3] Y. Ono, Catal. Today 81 (2003) 3.
[4] J. Libuda, M. Frank, A. Sandell, S. Andersson, P.A. Brühwiler, M. Bäumer, N. Mårtensson, H.-J. Freund, Surf. Sci. 384 (1997) 106.
[5] M. Heemeier, M. Frank, J. Libuda, K. Wolter, H. Kuhlenbeck, M. Bäumer, H.-J. Freund, Catal. Lett. 68 (2000) 19.
[6] A.Yu. Stakheev, W.M.H. Sachtler, J. Chem. Soc. Faraday Trans. 87 (1991) 3703.
[7] W.M.H. Sachtler, Z. Zhang, Adv. Catal. 39 (1993) 129.
[8] M. Vaarkamp, J.T. Miller, F.S. Modica, et al. Stud. Surf. Sci. Catal. 75 (1993) 809.
[9] V.L. Zholobenko, G.D. Lei, B.T. Carvill, et al. J. Chem. Soc. Faraday Trans. 90 (1994) 233.
[10] R.S. Weber, M. Boudart, P. Gallezot, Stud. Surf. Sci. Catal. 4 (1980) 415.
[11] D. Kubička, N. Kumar, T. Venäläinen, et al. J. Phys. Chem. B 110 (2006) 4937.
[12] J.I. Villegas, D. Kubička, H. Karhu, et al. J. Mol. Catal. A 264 (2007) 192.
[13] G.N. Vayssilov, B.C. Gates, N. Rösch, Angew. Chem. Int. Ed. 42 (2003) 1391.
[14] G.N. Vayssilov, N. Rösch, Phys. Chem. Chem. Phys. 7 (2005) 4019.
[15] G.P. Petrova, G.N. Vayssilov, N. Rösch, Chem. Phys. Lett. 444 (2007) 215.
[16] E.A. Ivanova Shor, V.A. Nasluzov, A.M. Shor, J. Phys. Chem. C 111 (2007) 12340.
[17] P. Treesukol, K. Srisuk, J. Limtrakul, T.N. Truong, J. Phys. Chem. B 109 (2005) 11940.
[18] M.N. Mikhailov, L.M. Kustov, V.Z. Mordkovich, Russ. Chem. Bull. 56 (2007) 397.
[19] M.N. Mikhailov, L.M. Kustov, V.B. Kazansky, Catal. Lett. 120 (2008) 8.
[20] A.D. Becke, J. Chem. Phys. 98 (1993) 5648.
[21] C. Lee, W. Yang, R.G. Parr, Phys. Rev. B 37 (1988) 785.
[22] S.H. Vosko, L. Wilk, M. Nusair, Can. J. Phys. 58 (1980) 1200.
[23] W.J. Stevens, M. Krauss, H. Basch, P.G. Jasien, Can. J. Chem. 70 (1992) 612.
[24] A.A. Granovsky, PC GAMESS version 7.1, http://classic.chem.msu.su/gran/gamess/index.html.
[25] M.W. Schmidt, K.K. Baldridge, J.A. Boatz, et al. J. Comput. Chem. 14 (1993) 1347.
[26] NBO 4.M. E.D. Glendening, J.K. Badenhoop, A.E. Reed, J.E. Carpenter, F. Weinhold, Theoretical Chemistry Institute, University of Wisconsin, Madison, WI, 1999.
[27] S.I. Gorelsky, AOMix: program for molecular orbital analysis, http://www.sg-chem.net/, York University: Toronto, Canada, 1997.
[28] S.I. Gorelsky, A.B.P. Lever, J. Organomet. Chem. 635 (2001) 187.